Peer-reviewed version available at Water 2018, 10, 297; doi:10.3390/w10030297

Article

Water level measurements from drones

Ridolfi E., Manciola P.
University of Perugia, Department of Civil and Environmental Engineering, Perugia, Italy.
* Correspondence: elena.ridolfi@unipg.it; Tel.: +39 075.5853619 (office)

Received: date; Accepted: date; Published: date

Abstract: Unmanned Aerial Vehicles (UAVs) are now filling in the gaps between spaceborne and ground-based observations and enhancing the spatial resolution and temporal coverage of data acquisition. In the realm of hydrological observations, UAVs have a key role to quantitatively characterize the surface flow allowing for remotely accessing the water body of interest. In this paper we propose a technology which uses a sensing platform encompassing a drone and a camera to determine the water level. The images acquired my means of the sensing platform are then analyzed using the Canny method to detect the edges of water level and of Ground Control Points (GCPs) used as reference points. The water level is then retrieved from images and compared to a benchmark value obtained by a traditional device. The method is tested at four locations in an artificial lake in central Italy. Results are encouraging as the overall mean error between estimated and true water level values is around 0.02 m. This technology is well suited to improve hydraulic modeling and thus provide a reliable support to flood mitigation strategies also in uneasy-to-access environments.

Keywords: water level measurement; surface hydrology; unmanned aerial vehicle; drone; dam.

1. Introduction

In recent years the awareness of the importance of spatial and temporal variation of open water level has increased [1]. The knowledge of water level provides information about the variability of water bodies and thus have a key role for monitoring and management of water resources. For instance, validation and calibration of hydraulic models [2–4] and of flood forecasting models [5,6] rely on accurate water level estimates in rivers. Water level measurements are at the basis of flood risk mitigation strategies as the understanding of the flood inundation extent allows for the construction of a resilient environment [7,8]. Water levels are usually monitored by means of gauging stations. However, water level sensors are characterized by some drawbacks as for instance their pointwise measurements and their limited use in uneasy-to-access environments. Moreover, their accuracy can be affected by several issues such as severe storm events and systematic errors associated with the sensors itself [9]. Recently, substantial efforts have been headed to the development of non-invasive technologies to monitor water level. For instance, Hut et al. [10] proved that the Wiimote device belonging with the Nintendo® Wii™ game system could be used to estimate water level values. Remote sensors based methods such as ENVISAT and ERS-2 satellite missions allowed for estimating water level of inland lakes with high precision (e.g. [11,12]). Nevertheless, spaceborne sensors are affected by limitations that restrict their ability to measure the temporal and spatial variation of the water level such as fixed orbit configurations and coarse temporal resolution. An overview on the wide variety of existing sensors can be found in Fraden [13]. Recently, there has been an increasing interest in the development of image-based technologies to determine water level values (e.g. [14]). Griesbaum et al. [15] developed a low-cost method to estimate flood elevation and inundation depth based on user-generated flood images. As a drawback, image-based systems can be affected by lighting changes, camera movement, condensation on the lens [16,17]. The spreading use of unmanned aerial vehicles (UAVs) paved the way of the integration of drone technology and optical sensing aiming at quantitatively estimating

hydraulic data such as inundated areas [18]; surface flow measurements (e.g., [19]); water level estimations [14]. A drone leads to a non-invasive monitoring of water bodies and it is an efficient tool in difficult-to-access environments. Moreover, the use of a drone helps to face and solve the issues associated to traditional gauging methods allowing the user for an accurate measurements of the water level [9]. In this paper we propose a sensing platform which couples a drone and a camera to estimate the water level of an artificial lake. Water level monitoring has a key role in lakes management as lakes are used as reservoirs for drinking water and for hydroelectric power generation among the other purposes. A drop of lake's level can cause severe damages to the ecosystem and to local economy. The cause of lakes decline can be found not only in a changing climatic forcing but also in a wrong management of the water resources [20–23]. As among the causes of dam break we can list extreme rainfall events that sharply increase the water level (e.g. [24,25]), a proper management of the water level in dam reservoirs is of utmost importance. Moreover, dams and reservoirs plays a major role in altering hydrological variability [26] and affecting hydrological extremes [27] thus modifying the frequency, magnitude and distribution of floods and droughts [28]. It is worth noting that despite the method presented in this paper has been tested on the water level of a dam lake, it can find application to any water body such as rivers, flood inundation areas, glaciers, coasts and river estuaries. This image-based technology is well suited in the framework of the Prediction in Ungauged Basins decade [29] as this method can be used to retrieve hydraulic data in ungauged sites [30]. The drone help to overcome the problems due to the use of traditional static sensors which require costly maintenance and personnel and thus can be deployed in limited number [31,32]. Water level measurements can then be used to improve hydraulic modeling of rivers to support flood risk mitigation plans. Only few studies aim at estimating water depth from flood data acquired during the flood event itself (e.g.[33,34]), while flood-level is often retrieved using remote-sensing data in the aftermath of the event for post-event flood simulations (e.g. [35,36]). However, there still remains a lack of approaches to access information about the flood level and extent from images shot during the event itself. In this framework, a drone-based approach allows for accessing flood level information during the flood event itself providing an unique support to flood mitigation actions. As a complement to traditional documentation systems, the amount of volunteered hydraulic information are now becoming popular [37]. Recent studies shown the potential of approaches to estimate the flood extent and level from post-event flood images shot by volunteers (e.g. [38,39]). However, crowdsourced data ca be characterized by gaps in time and space due to the uneven distribution of engaged citizens [40]. The use of a drone can offer a unique opportunity to overcome these issues and thus to support citizen observatories activities.

This paper proposes a sensing platform allowing for remote sensing and accessing the water level. The platform enables the collection of hydraulic information also in hostile situations such as during the occurrence of a flood event and during adverse atmospheric conditions. This approach is expected to provide a substantial support to monitoring and management of water bodies.

The paper is organized as follow. First, the case study site is introduced and the aerial sensing platform is described. Since the image-based technique presented here requires the acquisition of ground control points (GCPs), the topographic survey is detailed together with the GCPs deployment. Then, the procedure to determine water level values from images is presented and then assessed comparing estimated water level values with the benchmark value. Results are discussed together with the analysis of the sources of uncertainty.

2. Materials and Methods

In this section we detail the aerial sensing platform used in the experiments and the case study area where the survey was performed. Then, we provide details on the procedure for the airborne water level measurements.

2.1. Case study site and experimental set-up description

The aerial sensing platform is a HIGHONE 4HSEPRO quadrotor mounting a gimbal system and a SONY Alpha 7R, 36.4 Mpix Full frame camera oriented with its axis along the perpendicular. The gimbal compensates drone vibrations due to flight operations and to the wind. The lens is a 35mm f/9; the camera focus, after being tested on a portion of the structure, was set to infinity during the survey. The test case study is the Ridracoli lake, an artificial lake generated by the homonymous dam in Emilia Romagna Region, central Italy, Figure 1. The Ridracoli dam is characterized by a double-curvature arch-gravity structure with a maximum height of 103.5 m and a crest length of 432 m at 561 m a.s.l.. The lake extends for about 5 km in two branches. The catchment area is 88.49 km^2 and the maximum water volume in the retention basin equals 33.06 Mm^3. The reservoir is the main drinking water supply of Romagna Region, providing from about 7.5 Mm^3/month of discharge in winter up to about 12 Mm^3/month in summer to a million resident customers, tourists and food industries [41]. The reservoir has a crucial role in reducing the pumping from underground sources and in providing water supply to the coast affected by subsidence and saline ingression into aquifers.

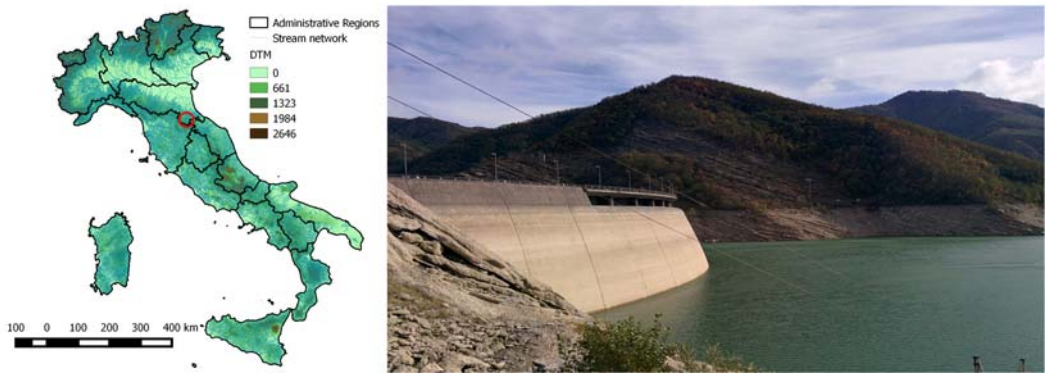

Figure 1. The test case study area is located in the Emilia Romagna Region, Central Italy. The red circle identify the location of the area, left panel. The experiment is performed at the Ridracoli lake, artificially created by the construction of the homonymous dam, right panel.

2.2. Ground control points acquisition

The technique presented in this paper to measure water level encompasses the need for ground control points (GCPs). GCPs drive the procedures of orthorectification and calibration of the images and are used as reference points to retrieve the water level values. The GCPs have a squared shape with a width of 0.40 m. In two different months (i.e. August and October 2015), sixty regularly–spaced GCPs were deployed on three rows on the upstream face of the dam. In this study we used the GCPs deployed on the lower row during October 2015 using a boat. The hydrostatic level of the time equaled 533.65 m a.s.l..

The identification of GCPs is one of the major sources of uncertainty after seeding density [42]. Therefore, the acquisition of GCPs coordinates has a crucial role in the experimental set-up. The coordinates of the GCPs were acquired through a traditional technique by means of a Total Station TS30 Leica-Geosystems. To this end, a pre-existing geodetic network consisting of four vertices materialized by little pillars was used. The coordinates of each GCP were estimated along the three directions. The standard deviation of each point is lower than 1 cm along the three directions. The mean value of all standard deviations equals 1.0 cm, 1.0 cm and 0.8 cm along the three directions, respectively. For a detailed description of the traditional topographic survey, the reader can refer to Buffi et al. [43,44]. The deployment of GCPs could represent one major pitfall of this technique, especially in areas with limited accesses. However, it is possible to use as reference point any point of known coordinates such as georeferenced point on a bridge pier. Furthermore, a methodology to address the need for ground control points is shown by Tauro et al. [19].

2.3. Image processing description

The images were shot at a distance of about 15 m from the dam; the Ground Sample Distance (GSD) equals 2.1 mm. The images are shot every 1.87 seconds and the images overlap by more than 70%. Each image size is 7360x4912 pixels with a resolution of 350 dpi. The camera positions on the upstream face of the dam where the water level was retrieved are shown in Figure 2. Every image is characterized by a minimum of four GCPs to allow for the orthorectification procedure [45].

After images acquisition, orthorectification was performed to eliminate distortions introduced by the angled camera and to calibrate image dimensions. The orthorectification procedure encompasses the following steps. First, control points such as GCPs are identified in the images. Control points associate an image point with a 3D world position (i.e. longitude, latitude and height acquired by the total station). Then, using bundle adjustment, the position and orientation of each image is estimated. Orthorectification is preformed using the estimated positions and orientations. Digital images are processed and orthorectified by means of the Hugin software [46] to obtain a high resolution RGB ortho-mosaic. Hugin is an open, easy-to-use cross platform panoramic imaging toolchain based on a free suite of programs and libraries (i.e. Panorama Tools; [47,48]). After orthorectification, the images are blended and projected onto a surface to provide the final mosaic [49]. Rectilinear projection is used to reconstruct the position of the camera and the geometry, assuming that the upstream face of the dam is mostly flat, so that all control points lie on a planar surface [50].

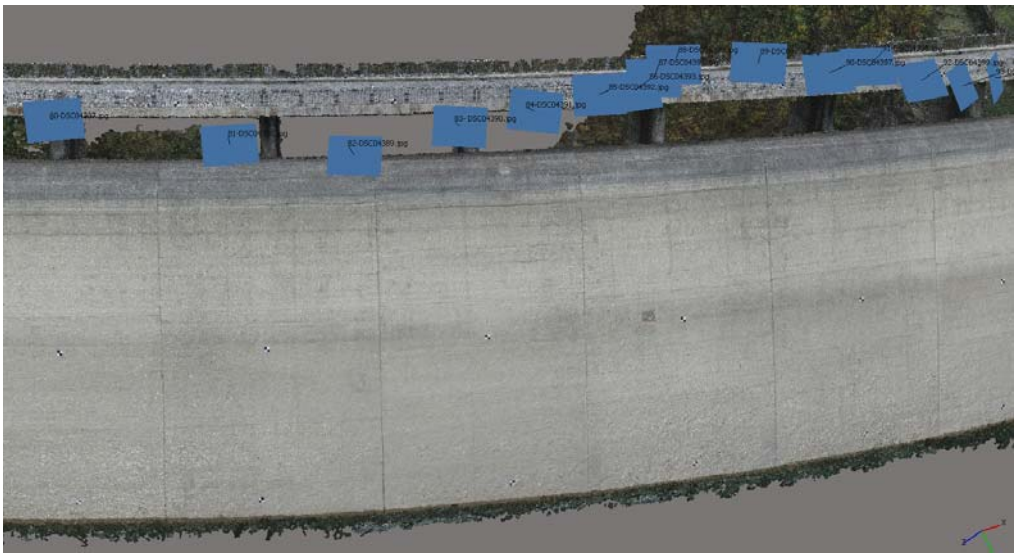

Figure 2. Camera positions in blue on a three dimensional model of the dam realized with Agisoft Photoscan® (v. 1.2.4).

2.4. Water level experimental procedure

The drone is flown above the water flowing through the upstream face of the dam. The frames used to estimate the water level values are the images shot at the upstream face where eight free spillway gates open to allow for the overflow of the dam, Figure 3a and b. The water level was estimated at four different locations to test the goodness of the procedure, Figure 3c. First, the water level is detected in the region of interest on the ortho-mosaic image where the water draws a dark line against a flat background. It is interesting to notice that there is a light grey shade on the dam surface due to a preexisting water level into the reservoir, Figure 3c. Therefore, it is necessary to pay attention to the identification of the water level to be accurate. The procedure to determine the water level value encompasses the following steps. First, the image is transformed into a grayscale image. Second, the edge detection operation is performed by means of the Canny method [51]. The Canny method finds edges by looking for local maxima of the gradient of the gray scale. The edge function calculates the gradient using the derivative of a Gaussian filter. This method uses two thresholds to detect strong and weak edges. By using two thresholds, the Canny method filters out the noise more than the other methods and can easily detect true weak edges. Nevertheless, anomalous edges can

still remain such as lines due to change in concrete color, to ashlars, etc. These anomalous edges are disregarded after the application of the filter. The minimum and maximum threshold values are equal to 0.019 and 0.047, respectively. GCP and water level edges are thus identified. Then, the water level line in pixel coordinates is calibrated to real world coordinates using as benchmark the center of each one of the four GCPs. The water level retrieved from the images shot by the sensing platform is then compared with a benchmark value. The benchmark is obtained from a spring balance which measures the weight of a water column and returns the corresponding water level of the lake. The wind speed at the time of the airborne flight generated a mild surface waviness allowing us to test the procedure also in adverse meteorological conditions.

Figure 3. Panels a) and b) two images shot at the upstream face of the dam, prior to orthorectification. Panel c) enlargement of a portion of the orthorectified image showing three of the four ground control points used to estimate the water level.

3. Results and discussion

The measurement procedure leads to determine the distance between each GCP and the edge of the water level. Several distance measurements are performed to take into account the uncertainty affecting the water level edge detection. Indeed, the water level line cannot be sharply identified because of different sources of uncertainty. The combination of the waves and of both angle and intensity of the incoming light source (e.g. sun, clouds) creates the sharp change in pixel gray scale in an image. Gilmore [52] investigated different sources of uncertainty affecting water level estimates from images. Besides the uncertainties associated to the local environment as the change in lighting, other sources of uncertainty are associated with the image quality such as the image focus, image resolution, perspective, and lens distortion. The images were processed as explained in Sect. 2.3 to eliminate distortion or perspective. Despite the high resolution of the images, there are limitations due to pixelization. Notably, the uncertainty in the water level estimates decreases as the resolution of the image increases. We used images with very high resolution, however, the effect of pixelization cannot be cut off completely.

The water level estimated at four GCPs on the upstream face of the dam by means of the aerial platform are compared with the water level reference value. The errors between the estimated water level values and the benchmark one are computed. To provide a quantitative indication of the procedure skill at estimating the water level value, we determined the mean absolute error (MAE) between observed and estimated values, the root mean squared error (RMSE) and the percentage BIAS. The MAE provides an estimate of the overall agreement between observed and estimated water level values. It is defined as:

Preprints (www.preprints.org) | NOT PEER-REVIEWED | Posted: 10 January 2018 doi:10.20944/preprints201801.0093.v1

Peer-reviewed version available at Water 2018, 10, 297; doi:10.3390/w10030297

$$\mathrm{MAE} = \frac{1}{N}\sum_{i=1}^{N}\left|W_{\mathrm{obs}} - W_{\mathrm{est},i}\right|, \quad (1)$$

where W_{obs} and W_{est} are water level values observed and estimated at a specific GCP, while N is the number of measurements performed using each GCP as fiducial and equals 40.

The RMSE is a non-negative metric without upper bound. A perfect estimation of the water level value would result in RMSE equaling zero. It is defined as:

$$\mathrm{RMSE} = \sqrt{\frac{1}{N}\sum_{i=1}^{N}\left(W_{\mathrm{obs}} - W_{\mathrm{est},i}\right)^2}. \quad (2)$$

RMSE is estimated in squared differences and thus it is biased in favor of high magnitude error, while it is insensitive to low magnitude ones. It is thus more sensitive to occasional large errors.

The BIAS represents the mean difference between observed and simulated values, in this paper it is presented in percentage:

$$\mathrm{BIAS}\cdot\% = \frac{1}{N}\sum_{i=1}^{N}\left(\frac{W_{\mathrm{obs}} - W_{\mathrm{est},i}}{W_{\mathrm{obs}}}\right)\cdot 100. \quad (3)$$

Estimated water level values result in line with the benchmark one, Table 1.

Table 1. Mean absolute error (MAE) between observed and estimated values, the root mean squared error (RMSE) and the percentage BIAS are reported for each ground control point (GCP).

ID GCP	MAE [m]	RMSE [m²]	BIAS [%]
1	0.045	0.047	0.008
2	0.012	0.015	0.000
3	0.031	0.038	0.005
4	0.051	0.062	0.005

The MAE evaluates all deviations from the observed value, in both an equal manner and regardless of the sign. As expected, the RMSE is similar to the MAE in magnitude. The amount of which the RMSE is larger than MAE is an indicator of the magnitude to which outliers exist in the data set [53]. The BIAS provides an indication of the extent of errors in percentage. The three estimation metrics allow us to draw encouraging considerations on the robustness and reliability of the proposed methods. To better visualize the distribution of errors, the boxplot of errors between estimated and observed water level values at each GCP is presented in Figure 4. The central mark indicates the median, and the bottom and top edges of the box indicate the 25th and 75th percentiles, respectively. The whiskers extend to the most extreme data values not considered outliers. The median error ranges between -0.01 m (i.e. at GCP 2) and 0.045 m (i.e. at GCP 1), while the mean deviation from the median is of ±0.02 m for the first three GCPs. The fourth GCP is characterized by a higher deviation as it is around ±0.06 m. The rationale of this result is due to the fact that at GCP 4, the perspective affects the measurements. This test was performed to understand which is the effect of the perspective on water level measurements from images.

Preprints (www.preprints.org) | NOT PEER-REVIEWED | Posted: 10 January 2018 doi:10.20944/preprints201801.0093.v1

Peer-reviewed version available at Water 2018, 10, 297; doi:10.3390/w10030297

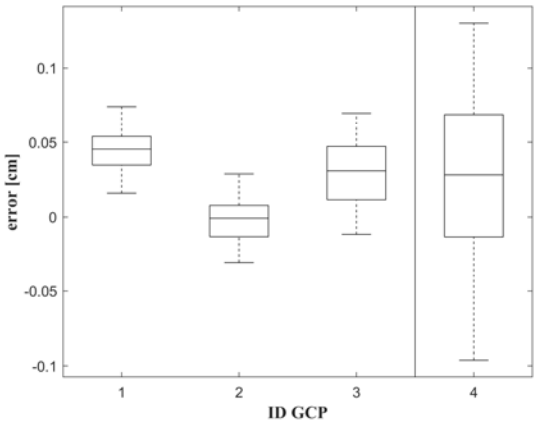

Figure 4. Boxplot of errors between estimated and observed water level values at the four Ground Control Points (GCPs).

The overall agreement of estimated water level values is good as the maximum error at each GCP is much lower than the sensibility of hydraulic models such as HEC-RAS (i.e. 0.20 m; [2]). This result paves the way to the use of water level estimates for calibration and validation of hydraulic models.

In agreement with the analysis performed by Gilmore et al. [52], the major sources of uncertainty are found to be the perspective and the pixelization, while the scale of the experiment allowed us to get rid of the effect of meniscuses which water forms at the contact with the background. It is worth underlining that the water surface waviness can affect substantially the water level estimates as waves ripple the water causing a blurry water level edge. Nevertheless, results are encouraging since image-based method compared favorably to the traditional technique. Results confirm that the method presented here has the potential to be used also in other scenarios providing reliable water level estimates.

5. Conclusions

In this work we propose a novel water level measurement concept based on the combination of an unmanned aerial vehicle and optical methods. The analysis of the images shot during the experiment demonstrates that the drone is compatible with the hydraulic measurements. A gimbal system compensates drone vibrations ensuring the stability of the drone and thus the quality of the images. It is worth noting that despite wind generated ripples affecting the water surface, the water level estimates were accurate confirming the robustness of the procedure. The main sources of uncertainty are found to be the pixelization of images and the perspective, nevertheless, results are encouraging and shows the potential of image-based measurements. The image analysis procedure is rapid and inexpensive as it is performed through an open source software (i.e. Hugin) allowing for an accurate estimation of the water level.

The sensing platform paves the way for unsupervised rapid observations in large scale hydrological systems. This apparatus can support flood inundation mapping as it allows an efficient event survey. The knowledge of the flood inundation extent and the water level values in the flooded area is crucial to support flood risk mitigation strategies. Moreover, the use of drones can be of great interest in ungauged sites where water level values and then discharges are retrieve by means of regionalization procedures that allow for information to be transferred from a hydrologically similar river basin. Image-based procedures relying on the use of a camera are now spreading, nevertheless it is not an easy task to retrieve hydraulic information in inaccessible areas. The use of a drone allows for overcoming this issue providing accurate information. Moreover, unmanned aerial vehicle can improve crowdsourced data collection, supporting citizen observatories lowering data uncertainty and filling in the significant gap due to areas with limited access.

Acknowledgments: The authors would like to express their sincere gratitude to Giulia Buffi who participated to the ground control points deployment, to Barberini who supported the acquisition of the drone images and Silvia Grassi, who directed the acquisition of the topographic data. Romagna Acque Società delle Fonti S.p.A. and its CEO Eng. Andrea Gambi are gratefully acknowledged for the access to the Ridracoli dam. This work was supported by the Italian Ministry of Education, University and Research under PRIN grant No. 20154EHYW9 "Combined numerical and experimental methodology for fluid structure interaction in free surface flows under impulsive loading".

Author Contributions: Both Authors equally contributed to any step from conceiving this work to analyzing results. E.R. wrote the paper.

Conflicts of Interest: The authors declare no conflict of interest.

References

1. Alsdorf, D. E.; Rodriguez, E.; Lettenmaier, D. P. Measuring surface water from space. *Rev. Geophys.* **2007**, *45*, 1–24.

2. Ridolfi, E.; Alfonso, L.; Di Baldassarre, G.; Dottori, F.; Russo, F.; Napolitano, F. An entropy approach for the optimization of cross-section spacing for river modelling. *Hydrol. Sci. J.* **2013**, *59*, 126–137.

3. Ridolfi, E.; Alfonso, L.; Di Baldassarre, G.; Napolitano, F. Optimal cross-sectional sampling for river modelling with bridges: An information theory-based method. In *AIP Conference Proceedings*; 2016; Vol. 1738.

4. Langhammer, J.; Bernsteinová, J.; Miřijovský, J. Building a High-Precision 2D Hydrodynamic Flood Model Using UAV Photogrammetry and Sensor Network Monitoring. *Water* **2017**, *9*, 861.

5. Montesarchio, V.; Napolitano, F.; Rianna, M.; Ridolfi, E.; Russo, F.; Sebastianelli, S. Comparison of methodologies for flood rainfall thresholds estimation. *Nat. Hazards* **2014**, *75*, 909–934.

6. Ridolfi, E.; Montesarchio, V.; Rianna, M.; Sebastianelli, S.; Russo, F.; Napolitano, F. Evaluation of rainfall thresholds through entropy: Influence of bivariate distribution selection. *Irrig. Drain.* **2013**, *62*.

7. Di Baldassarre, G.; Schumann, G.; Bates, P. D.; Freer, J. E.; Beven, K. J. Flood-plain mapping: a critical discussion of deterministic and probabilistic approaches. *Hydrol. Sci. J.* **2010**, *55*, 364–376.

8. Ridolfi, E.; Yan, K.; Alfonso, L.; Di Baldassarre, G.; Napolitano, F.; Russo, F.; Bates, P. D. An entropy method for floodplain monitoring network design. In *AIP Conference Proceedings*; 2012; Vol. 1479.

9. Tauro, F.; Porfiri, M.; Grimaldi, S. Surface flow measurements from drones. *J. Hydrol.* **2016**, *540*, 240–245.

10. Hut, R. W.; Weijs, S. V.; Luxemburg, W. M. J. Using the Wiimote as a sensor in water research. *Water Resour. Res.* **2010**, *46*, 1–5.

11. Medina, C. E.; Gomez-Enri, J.; Alonso, J. J.; Villares, P. Water level fluctuations derived from ENVISAT Radar Altimeter (RA-2) and in-situ measurements in a subtropical waterbody: Lake Izabal (Guatemala). *Remote Sens. Environ.* **2008**, *112*, 3604–3617.

12. Munyaneza, O.; Wali, U. G.; Uhlenbrook, S.; Maskey, S.; Mlotha, M. J. Water level monitoring using radar remote sensing data: Application to Lake Kivu, central Africa. *Phys. Chem. Earth, Parts A/B/C* **2009**, *34*, 722–728.

13. Fraden, J. *Handbook Of Modern Sensors: Physics, Designs, And Applications*; 3rd ed.; Springer, New York, 2004.

14. Bandini, F.; Jakobsen, J.; Olesen, D.; Reyna-Gutierrez, J. A.; Bauer-Gottwein, P. Measuring water level in rivers and lakes from lightweight Unmanned Aerial Vehicles. *J. Hydrol.* **2017**.

15. Griesbaum, L.; Marx, S.; Höfle, B. Direct local building inundation depth determination in 3-D point clouds generated from user-generated flood images. *Nat. Hazards Earth Syst. Sci.* **2017**, *17*, 1191–1201.

16. Iwahashi, M.; Udomsiri, S.; Imai, Y.; Muramatsu, S. Water Level Detection for Functionally Layered Video Coding. In *2007 IEEE International Conference on Image Processing*; IEEE, 2007; p. II-321-II-324.

17. Yu, J.; Hahn, H. Remote Detection and Monitoring of a Water Level Using Narrow Band Channel. *J. Inf. Sci. Eng.* **2010**, *26*, 71–82.

18. Feng, Q.; Liu, J.; Gong, J. Urban Flood Mapping Based on Unmanned Aerial Vehicle Remote Sensing and Random Forest Classifier—A Case of Yuyao, China. *Water* **2015**, *7*, 1437–1455.

19. Tauro, F.; Porfiri, M.; Grimaldi, S. Orienting the camera and firing lasers to enhance large scale particle image velocimetry for streamflow monitoring. *Water Resour. Res.* **2014**, *50*, 7470–7483.

20. Awange, J. L.; Sharifi, M. A.; Ogonda, G.; Wickert, J.; Grafarend, E. W.; Omulo, M. A. The Falling Lake Victoria Water Level: GRACE, TRIMM and CHAMP Satellite Analysis of the Lake Basin. *Water Resour. Manag.* **2008**, *22*, 775–796.

21. Swenson, S.; Wahr, J. Monitoring the water balance of Lake Victoria, East Africa, from space. *J. Hydrol.* **2009**, *370*, 163–176.

22. Manciola, P.; Di Francesco, S.; Biscarini, C.; Montesarchio, V. On the role of hydrological processes on the water balance of Lake Bolsena, Italy. *Lakes Reserv. Res. Manag.* **2016**, *21*, 45–55.

23. Pierleoni, A.; Bellezza, M.; Casadei, S.; Manciola, P. Multipurpose water use in a system of reservoirs. In *IAHS-AISH Publication*; 2007; pp. 107–116.

24. Biscarini, C.; Francesco, S. D.; Ridolfi, E.; Manciola, P. On the simulation of floods in a narrow bending valley: The malpasset dam break case study. *Water (Switzerland)* **2016**, *8*.

25. Rico, M.; Benito, G.; Salgueiro, A. R.; Díez-Herrero, A.; Pereira, H. G. Reported tailings dam failures: A review of the European incidents in the worldwide context. *J. Hazard. Mater.* **2008**, *152*, 846–852.

26. Ye, B.; Yang, D.; Kane, D. L. Changes in Lena River streamflow hydrology: Human impacts versus natural variations. *Water Resour. Res.* **2003**, *39*.

27. Baldassarre, G. Di; Martinez, F.; Kalantari, Z.; Viglione, A. Drought and flood in the Anthropocene : feedback mechanisms in reservoir operation. *Earth Syst. Dyn.* **2017**, *8*, 225–233.

28. Di Baldassarre, G.; Viglione, A.; Carr, G.; Kuil, L.; Yan, K.; Brandimarte, L.; Bloschl, G. Debates—Perspectives on socio-hydrology: Capturing feedbacks between physical and social processes. *Water Resour. Res.* **2015**, *51*, 4770–4781.

29. Sivapalan, M.; Takeuchi, K.; Franks, S. W.; Gupta, V. K.; Karambiri, H.; Lakshmi, V.; Liang, X.; Mcdonnell, J. J.; Mendiondo, E. M.; O'connell, P. E.; Oki, T.; Pomeroy, J. W.; Schertzer, D.; Uhlenbrook, S.; Zehe, E. IAHS Decade on Predictions in Ungauged Basins (PUB), 2003-2012: Shaping an exciting future for the hydrological sciences. *Hydrol. Sci. J.* **2003**, *48*, 857–880.

30. Ridolfi, E.; Rianna, M.; Trani, G.; L., A.; Di Baldassarre, G.; Napolitano, F.; Russo, F. A new methodology to define homogeneous regions through an entropy based clustering method. *Adv. Water Resour.* **2016**.

31. Alfonso, L.; Ridolfi, E.; Gaytan-Aguilar, S.; Napolitano, F.; Russo, F. Ensemble entropy for monitoring network design. *Entropy* **2014**, *16*.

32. Ridolfi, E.; Servili, F.; Magini, R.; Napolitano, F.; Russo, F.; Alfonso, L. Artificial Neural Networks and Entropy-based Methods to Determine Pressure Distribution in Water Distribution Systems. *Procedia Eng.* **2014**, *89*, 648–655.

33. Mason, D. C.; Giustarini, L.; Garcia-Pintado, J.; Cloke, H. L. Detection of flooded urban areas in high resolution Synthetic Aperture Radar images using double scattering. *Int. J. Appl. Earth Obs. Geoinf.* **2014**, *28*, 150–159.

34. Iervolino, P.; Guida, R.; Iodice, A.; Riccio, D. Flooding Water Depth Estimation With High-Resolution SAR. *IEEE Trans. Geosci. Remote Sens.* **2015**, *53*, 2295–2307.

35. Schumann, G. J.-P.; Neal, J. C.; Mason, D. C.; Bates, P. D. The accuracy of sequential aerial photography and SAR data for observing urban flood dynamics, a case study of the UK summer 2007 floods. *Remote Sens. Environ.* **2011**, *115*, 2536–2546.

36. Jung, Y.; Kim, D.; Kim, D.; Kim, M.; Lee, S. Simplified Flood Inundation Mapping Based On Flood Elevation-Discharge Rating Curves Using Satellite Images in Gauged Watersheds. *Water* **2014**, *6*, 1280–1299.

37. Wehn, U.; Rusca, M.; Evers, J.; Lanfranchi, V. Participation in flood risk management and the potential of citizen observatories: A governance analysis. *Environ. Sci. Policy* **2015**, *48*, 225–236.

38. Triglav-Čekada, M.; Radovan, D. Using volunteered geographical information to map the November 2012 floods in Slovenia. *Nat. Hazards Earth Syst. Sci.* **2013**, *13*, 2753–2762.

39. Narayanan, R.; Lekshmy, V. M.; Rao, S.; Sasidhar, K. A novel approach to urban flood monitoring using computer vision. In *Fifth International Conference on Computing, Communications and Networking Technologies (ICCCNT)*; IEEE, 2014; pp. 1–7.

40. Mazzoleni, M.; Alfonso, L.; Chacon-Hurtado, J.; Solomatine, D. Assimilating uncertain, dynamic and intermittent streamflow observations in hydrological models. *Adv. Water Resour.* **2015**, *83*, 323–339.

41. Romano, E.; Guyennon, N.; Bon, A. Del; Petrangeli, A. B.; Preziosi, E. Robust Method to Quantify the Risk of Shortage for Water Supply Systems. *Asce* **2017**, *22*.

42. Kim, Y. Uncertainty analysis for non-intrusive measurement of river discharge using image velocimetry, PhD thesis, Grad. Coll. of the Univ. of Iowa, The University of Iowa, Iowa City, Ia, 2006.

43. Buffi, G.; Manciola, P.; Grassi, S.; Gambi, A.; Barberini, M. Survey of the Ridracoli Dam: UAV – Based Photogrammetry and Traditional Topographic Techniques in the inspection of VerticalStructures. *Geomatics, Nat. Hazards Risk* accepted.

44. Buffi, G.; Manciola, P.; De Lorenzis, L.; Cavalagli, N.; Comodini, F.; Gambi, A.; Gusella, V.; Mezzi, M.; Niemeier, W.; Tamagnini, C. Calibration of finite element models of concrete arch-gravity dams using dynamical measures: the case of Ridracoli. *Procedia Eng.* **2017**, *199*, 110–115.

45. Hauet, A.; Kruger, A.; Krajewski, W. F.; Bradley, A.; Muste, M.; Creutin, J.-D.; Wilson, M. Experimental System for Real-Time Discharge Estimation Using an Image-Based Method. *J. Hydrol. Eng.* **2008**, *13*, 105–110.

46. Hugin Manual, 2013, http://hugin.sourceforge.net/docs/manual/Hugin.html. Accessed 30th December 2017.

47. Dersch, H. Panorama Tools: Open Source Software for Immersive Imaging. In *International VR Photography Conference*; Berkley, 2007.

48. Dersch, H. https://webuser.hs-furtwangen.de/~dersch/, Accessed 30th December 2017. *Artic. Softw. Hochschule Furtwangen Univ.* **2015**.

49. Szeliski, R. *Image Alignment and Stitching: A Tuto- rial, Technical Report, MSR-TR-2004-92. Microsoft Research, Redmond, WA*; 2004.

50. Venturi, S.; Di Francesco, S.; Materazzi, F.; Manciola, P. Unmanned aerial vehicles and Geographical Information System integrated analysis of vegetation in Trasimeno Lake, Italy. *Lakes Reserv. Res. Manag.* **2016**, *21*, 5–19.

51. Canny, J. A Computational Approach to Edge Detection. *IEEE Trans. Pattern Anal. Mach. Intell.* **1986**, *PAMI-8*, 679–698.

416 52. Gilmore, T. E.; Birgand, F.; Chapman, K. W. Source and magnitude of error in an inexpensive
417 image-based water level measurement system. *J. Hydrol.* **2013**, *496*, 178–186.

418 53. Dawson, C. W.; Abrahart, R. J.; See, L. M. HydroTest: A web-based toolbox of evaluation metrics
419 for the standardised assessment of hydrological forecasts. *Environ. Model. Softw.* **2007**, *22*, 1034–1052.

420